


**COVER PAGE**

***Document downloaded by @DAEL***

***Sun Nov 29 13:38:53 2026***
***For personal use***

When automatic English translation is provided, only the original document is authentic.
The EAA cannot be held responsible of any translation error

Bibliographical reference

*Analytical and Experimental Investigation on Thick Plates in Flexural Vibration*, He Xiping, Zhu Ting and Pan Xiaojuan, Acta Acustica **vol. 100** (Number 3), 2014, pp. 411-417

DOI
https://doi.org/10.3813/AAA.918720

**Acta Acustica united with Acustica**
**Vol. 100 (2014) 411 – 417**

DOI 10.3813/AAA.918720

# Analytical and Experimental Investigation on Thick Plates in Flexural Vibration

He Xiping[1)], Zhu Ting[2)], Pan Xiaojuan[1)]

[1)] Institute of Applied Acoustics, Shaanxi Normal University, Xian, 710062, China. Hexiping@snnu.edu.cn

[2)] Department of Ultrasound, Xijing Hospital, Fourth Military Medical University, Xi'an, 710032, China. zhuting66@163.com

**Summary**

A thin plate in flexural vibration, as a high power radiator driven by a longitudinal transducer at its center, has been widely used in the air due to its extensive radiation surface. In the wide field of high-power sonic and ultrasonic applications, the radiated plates being able to withstand higher mechanical strength are required. However, the mechanical strength of a thin plate seems insufficient, and a thick plate may be a good substitute. This paper refers specially to design of a thick plate in flexural vibration at certain operating frequency with its boundary conditions being free, simply supported and clamped. In this work, the analytical solutions of radial and transverse displacements, and the resonant frequency equations of a thick plate in flexural vibration are proposed and derived based on Mindlin plate theory. The calculated frequencies by the presented analytical method are in good agreement with the ones by using finite element method, and validated by experimental tests.

**PACS no. 43.40.+r, 43.40.Rj**

## 1. Introduction

A thin plate in flexural vibration, driven by a longitudinal transducer at its center, has been in use for a number of years for the generation of ultrasounds, due to its extensive radiation surfaces to offering good impedance match to air [1, 2, 3, 4]. In these applications, the derived frequency equations for design of the plates in flexural vibration are all based on the classical thin plate theory [5, 6], that is the "Hypothesis of Kirchhoff". The hypothesis of Kirchhoff's straight-line neglects shear deformation, and enlarges rigidity, and is mainly applicable for design of thin plates with small ratio of thickness to length. The limitations of the classical thin plate will be significantly occurred as the ratio gradually increases (mostly greater than 1/5) [7].

The wide field of high-power sonic and ultrasonic applications, which is presently known as macrosonics, requires the radiated plate to be able to withstand a higher mechanical strength within the vibrating system as the above mentioned. For example, in liquid processes, which are generally based on cavitation effects, may require reaching a certain sound pressure level (cavitation threshold) throughout a volume; in gas processes, which are usually based on radiation pressure and particle velocity, may require adequate vibrational amplitudes and treatment times; and in solid processes, generally carried out directly on the material, high stresses are needed to produce friction, heat and other suitable secondary effects [8, 9, 10, 11, 12]. The mechanical strength of a thin plate seems insufficient, and a thick plate may be a good substitute. To extend the application to thick plates, Mindlin plate theory, also called shear deformation theory is used, in which the effect of the shear deformation and the rotary inertia cannot be omitted [13].

For high-power application, how to design a thick plate radiator with its boundary conditions being free, simply supported and clamped, is our issues of concern. In this paper, the analytical solutions of radial and transverse displacements, and the resonant frequency equations of a thick plate in flexural vibration are proposed and derived based on Mindlin plate theory. The results obtained by the presented method are in good agreement with those of by using finite element method and validated by experimental tests.

Received 23 February 2013,
accepted 3 January 2014.

## 2. Flexural vibration of thick plates

### 2.1. Mindlin plate theory

In the analysis of a thick plate, it is assumed that (a) there is no "thickness stretch" of the plate; (b) straight lines that are perpendicular to the mid-plane in the undeformed state remain straight in the deformed state even though they may not remain perpendicular to the mid-plane. Taking the origin of the cylindrical coordinate system is at the center of the median plane of a thick plate. According to this theory, the displacement fields of the plate in the cylindrical

© S. Hirzel Verlag · EAA

coordinate are given as [13]

$$\begin{aligned} u_r &= z\psi_r(r,\theta,t), \\ u_\theta &= z\psi_\theta(r,\theta,t), \\ u_z &= \overline{w}(r,\theta,t). \end{aligned} \tag{1}$$

Radius and thickness of the thick plate, respectively, are $a$ and $h$. Where $u_r$, $u_\theta$ and $u_z$, respectively, are the displacements in the radial $r$-direction, tangential $\theta$-direction and transverse $z$-direction of the plate; $w$ is the transverse displacement of the mid-plane; $\psi_r$ and $\psi_\theta$ are the rotations of vertical lines perpendicular to the mid-plane, measured on the $z$–$r$ and $z$–$\theta$ planes, respectively.

Here,

$$\begin{aligned} \psi_r &= \big(\sigma_1 - 1\big)\frac{\partial \overline{w}_1}{\partial r} + \big(\sigma_2 - 1\big)\frac{\partial \overline{w}_2}{\partial r} + \frac{1}{r}\frac{\partial H}{\partial \theta}, \\ \psi_\theta &= \big(\sigma_1 - 1\big)\frac{1}{r}\frac{\partial \overline{w}_1}{\partial \theta} + \big(\sigma_2 - 1\big)\frac{1}{r}\frac{\partial \overline{w}_2}{\partial \theta} + \frac{\partial H}{\partial r}, \\ \overline{w} &= \overline{w}_1 + \overline{w}_2. \end{aligned} \tag{2}$$

The displacement functions $\overline{w}_1$ and $\overline{w}_2$, respectively, satisfy

$$\begin{aligned} \big(\nabla^2 + \delta_1^2\big)\overline{w}_1 &= 0, \\ \big(\nabla^2 + \delta_2^2\big)\overline{w}_2 &= 0, \\ \big(\nabla^2 + P^2\big)H &= 0, \end{aligned} \tag{3}$$

where

$$\begin{aligned} \delta_1^2, \delta_2^2 &= \frac{1}{2}\delta_0^4\left[R + S \pm \sqrt{(R-S)^2 + 4\delta_0^4}\right], \\ \sigma_1, \sigma_2 &= \frac{\delta_1^2, \delta_2^2}{R\delta_0^4 - S^{-1}}, \quad P^2 = 2\frac{R\delta_0^4 - S^{-1}}{1-\nu}. \end{aligned}$$

Here, $R = h^2/12$, $S = D/k^2Gh$, $\delta_0^4 = \rho\omega^2 h/D$, $D = Eh^3/12(1-\nu^2)$, $k^2 = \pi/12$. $\rho$, $\omega$ and $D$, respectively, are density, angular frequency and bending stiffness constant. The expressions of bending moments $M_r$ and $M_\theta$, torque moment $M_{r\theta}$ and transverse shear forces $Q_r$ and $Q_\theta$, can be respectively expressed as

$$\begin{aligned} M_r &= D\left[\frac{\partial \psi_r}{\partial r} + \frac{\nu}{r}\left(\psi_r + \frac{\partial \psi_\theta}{\partial \theta}\right)\right], \\ M_\theta &= D\left[\frac{1}{r}\left(\psi_r + \frac{\partial \psi_\theta}{\partial \theta}\right) + \nu\frac{\partial \psi_r}{\partial r}\right], \\ M_{r\theta} &= \frac{D}{2}(1-\nu)\left[\frac{1}{r}\left(\frac{\partial \psi_r}{\partial \theta} - \psi_\theta\right) + \frac{\partial \psi_\theta}{\partial r}\right], \\ Q_r &= k^2Gh\left(\psi_r + \frac{\partial \overline{w}}{\partial r}\right), \\ Q_\theta &= k^2Gh\left(\psi_\theta + \frac{1}{r}\frac{\partial \overline{w}}{\partial \theta}\right). \end{aligned} \tag{4}$$

### 2.2. Frequency equations

For circular thick plates, vibration is axisymmetric to $z$ axis, the displacement in $\theta$-direction need not be considered. $u_r$, $u_\theta$ and $w$ can be expressed as

$$\begin{aligned} u_r &= z\psi_r(r,t), \\ u_\theta &= 0, \\ \overline{w} &= \overline{w}(r,t). \end{aligned} \tag{5}$$

Here,

$$\begin{aligned} \psi_r &= \big(\sigma_1 - 1\big)\frac{\partial \overline{w}_1}{\partial r} + \big(\sigma_2 - 1\big)\frac{\partial \overline{w}_2}{\partial r}, \\ \overline{w} &= \overline{w}_1 + \overline{w}_2. \end{aligned} \tag{6}$$

The bending moment and transverse shear force are described as

$$\begin{aligned} M_r &= D\left[\frac{\partial \psi_r}{\partial r} + \frac{\nu}{r}\psi_r\right], \\ Q_r &= k^2Gh\left(\psi_r + \frac{\partial \overline{w}}{\partial r}\right). \end{aligned} \tag{7}$$

Equation (3) can be written as

$$\begin{aligned} \frac{\partial^2 \overline{w}_1}{\partial r^2} + \frac{1}{r}\frac{\partial \overline{w}_1}{\partial r} + \delta_1^2\overline{w}_1 &= 0, \\ \frac{\partial^2 \overline{w}_2}{\partial r^2} + \frac{1}{r}\frac{\partial \overline{w}_2}{\partial r} + \delta_1^2\overline{w}_2 &= 0. \end{aligned} \tag{8}$$

The solutions of equation (8) have the following expressions

$$\begin{aligned} \overline{w}_1 &= A_1 J_0(\delta_1 r) + B_1 N_0(\delta_1 r), \\ \overline{w}_2 &= A_2 J_0(\delta_2 r) + B_2 N_0(\delta_2 r), \end{aligned} \tag{9}$$

where $J_0(\delta_1 r)$ and $J_0(\delta_2 r)$ are Zeroth-order Bessel Functions, and $N_0(\delta_1 r)$ and $N_0(\delta_2 r)$ are Zeroth-order Neumann Functions, respectively, and the values of the constants $A_1$, $A_2$, $B_1$ and $B_2$ are determined by the boundary conditions of the thick plate. Substitution of equation (9) into equations (5) and (6), can be obtained as

$$\begin{aligned} \psi_r &= \delta_1\big(1-\sigma_1\big)\big[A_1 J_1(\delta_1 r) + B_1 N_1(\delta_1 r)\big] \\ &\quad + \delta_2\big(1-\sigma_2\big)\big[A_2 J_1(\delta_2 r) + B_2 N_1(\delta_2 r)\big], \\ \overline{w} &= A_1 J_0(\delta_1 r) + B_1 N_0(\delta_1 r) \\ &\quad + A_2 J_0(\delta_2 r) + B_2 N_0(\delta_2 r). \end{aligned} \tag{10}$$

Since the function $\overline{w}$ is infinite at $r = 0$, the coefficients $B_1$ and $B_2$ must be zero. Equation (10) can be simplified

$$\psi_r = A_1\delta_1\big(1-\sigma_1\big)J_1(\delta_1 r) + A_2\delta_2\big(1-\sigma_2\big)J_1(\delta_2 r), \tag{11}$$

$$\overline{w} = A_1 J_0(\delta_1 r) + A_2 J_0(\delta_2 r). \tag{12}$$

Substitution of equations (11) and (12) into equation (7) are given as

$$\begin{aligned} M_r &= A_1\delta_1\big(1-\sigma_1\big)\left[\delta_1 J_0(\delta_1 r) + \frac{\nu-1}{r}J_1(\delta_1 r)\right] \\ &\quad + A_2\delta_2\big(1-\sigma_2\big)\left[\delta_2 J_0(\delta_2 r) + \frac{\nu-1}{r}J_1(\delta_2 r)\right], \end{aligned} \tag{13}$$

$$Q_r = -\big[A_1\delta_1 J_1(\delta_1 r) + A_2\delta_2 J_1(\delta_2 r)\big]. \tag{14}$$

#### 2.2.1. Free boundary

The boundary conditions at $r = a$, for a free edge of a thick plate, are $Q_r(a) = 0$ and $M_r(a) = 0$. The frequency equation can be obtained from equations (13) and (14),

$$\begin{aligned} &A_1\delta_1\big(1-\sigma_1\big)\left[\delta_1 J_0(\delta_1 a) + \frac{\nu-1}{r}J_1(\delta_1 a)\right] \\ &+A_2\delta_2\big(1-\sigma_2\big)\left[\delta_2 J_0(\delta_2 a) + \frac{\nu-1}{r}J_1(\delta_2 a)\right] = 0, \end{aligned} \tag{15}$$

$$-\big[A_1\delta_1 J_1(\delta_1 a) + A_2\delta_2 J_1(\delta_2 a)\big] = 0. \tag{16}$$

Table I. The calculated resonant frequencies of the plates.

| | | Clamped | | | Free | | | Simply supported | | |
|---|---|---|---|---|---|---|---|---|---|---|
| h | n | $f_M$ | $f_K$ | $f_A$ | $f_M$ | $f_K$ | $f_A$ | $f_M$ | $f_K$ | $f_A$ |
| | 1 | 26.47 | 32.93 | 27.17 | 25.41 | 28.88 | 25.64 | 14.66 | 15.81 | 14.80 |
| 8 | 2 | 76.90 | 128.01 | 80.81 | 82.23 | 123.79 | 85.38 | 67.89 | 95.72 | 70.47 |
| | 3 | 135.05 | 287.24 | 145.72 | 144.24 | 282.74 | 154.15 | 130.39 | 238.98 | 139.70 |
| | 1 | 28.54 | 37.05 | 29.16 | 27.89 | 32.49 | 28.02 | 16.25 | 17.79 | 16.34 |
| 9 | 2 | 80.37 | 144.23 | 83.57 | 86.88 | 139.26 | 89.12 | 72.23 | 107.70 | 74.25 |
| | 3 | 139.26 | 323.15 | 147.29 | 148.40 | 318.08 | 155.02 | 135.68 | 268.86 | 142.50 |
| | 1 | 30.25 | 41.17 | 31.14 | 30.06 | 36.10 | 30.33 | 17.66 | 19.77 | 17.87 |
| 10 | 2 | 83.03 | 160.26 | 87.20 | 90.46 | 154.74 | 93.64 | 75.72 | 119.67 | 78.63 |
| | 3 | 142.36 | 359.05 | 153.04 | 150.59 | 353.43 | 158.80 | 139.62 | 298.73 | 149.09 |
| | 1 | 31.82 | 45.28 | 32.74 | 32.10 | 39.71 | 32.41 | 19.05 | 21.74 | 19.30 |
| 11 | 2 | 85.22 | 176.29 | 89.48 | 97.27 | 170.21 | 96.56 | 78.70 | 131.63 | 81.79 |
| | 3 | 144.64 | 394.96 | 155.39 | 150.55 | 388.77 | 157.80 | 142.57 | 328.60 | 152.24 |
| | 1 | 33.19 | 49.40 | 34.22 | 34.01 | 43.31 | 34.35 | 20.38 | 23.72 | 20.63 |
| 12 | 2 | 87.13 | 192.31 | 91.67 | 95.54 | 185.68 | 99.08 | 81.36 | 143.60 | 84.69 |
| | 3 | 146.22 | 430.86 | 157.84 | 149.40 | 424.11 | 155.71 | 145.23 | 358.47 | 159.63 |

After simplifying, the above equations can be written as

$$\frac{\sigma_2 J_1(\delta_2 a)}{\sigma_1 J_1(\delta_1 a)}\left(1-\sigma_1\right)\left[\delta_1 J_0(\delta_1 a)+\frac{\nu-1}{a}J_1(\delta_1 a)\right] = \left(1-\sigma_2\right)\left[\delta_2 J_0(\delta_2 a)+\frac{\nu-1}{a}J_1(\delta_2 a)\right]. \quad (17)$$

2.2.2. Simply supported boundary

The boundary conditions at $r = a$ for a simply supported edge of a thick plate, are $\overline{w}(a) = 0$ and $M_r(a) = 0$. The frequency equation can be obtained from equations (12) and (13),

$$A_1 J_0(\delta_1 a) + A_2 J_0(\delta_2 a) = 0, \quad (18)$$

$$A_1\delta_1\left(1-\sigma_1\right)\left[\delta_1 J_0(\delta_1 a)+\frac{\nu-1}{a}J_1(\delta_1 a)\right] + A_2\delta_2\left(1-\sigma_2\right)\left[\delta_2 J_0(\delta_2 a)+\frac{\nu-1}{a}J_1(\delta_2 a)\right] = 0. \quad (19)$$

After simplifying, the above equations can be written as

$$\frac{J_0(\delta_2 a)}{J_0(\delta_1 a)}\delta_1\left(1-\sigma_1\right)\left[\delta_1 J_0(\delta_1 a)+\frac{\nu-1}{a}J_1(\delta_1 a)\right] = \delta_2\left(1-\sigma_2\right)\left[\delta_2 J_0(\delta_2 a)+\frac{\nu-1}{a}J_1(\delta_2 a)\right]. \quad (20)$$

2.2.3. Clamped boundary

The boundary conditions at $r = a$, for a clamped edge of a thick plate, are $\overline{w}(a) = 0$ and $\psi_r(a) = 0$. The frequency equation can be obtained from equations (11) and (12)

$$A_1 J_0(\delta_1 a) + A_2 J_0(\delta_2 a) = 0, \quad (21)$$

$$A_1\delta_1\left(1-\sigma_1\right)J_1(\delta_1 a) + A_2\delta_2\left(1-\sigma_2\right)J_1(\delta_2 a) = 0. \quad (22)$$

After simplifying, the above equations can be written as

$$\delta_2\left(1-\sigma_2\right)J_1(\delta_2 a) = \frac{J_0(\delta_2 a)}{J_0(\delta_1 a)}\delta_1\left(1-\sigma_1\right)J_1(\delta_1 a). \quad (23)$$

## 3. Numerical calculations

To validate the analytical solutions from the above flexural vibration frequency equations, the first three corresponding frequencies of the vibrational modes of a thick plate with free, simply-supported and clamped boundary conditions are calculated by using finite element method. Taking the material of a thick plate is steel, its density $\rho = 7.8 \cdot 10^3\,\mathrm{kg/m^3}$, Poisson's ratio $\nu = 0.28$, Young's modulus $E = 21.6 \cdot 10^{10}\,\mathrm{N/m^2}$, and its shear modulus $G = 8.4 \cdot 10^{10}\,\mathrm{N/m^2}$. Taking the radius and thickness of the thick plate are $a = 25\,\mathrm{mm}$ and $h$ (it can be variable, as shown in Table I), respectively, and keeping the radius is constant, the first three calculated flexural resonant frequencies are shown in Table I. Here, $f_M$, $f_A$ and $f_K$ are the calculated frequencies by the presented analytical method, by using finite element method and by thin plate theory, respectively; and n denotes the modal order number. The unit of frequency is kHz.

From Table I, the calculated resonant frequencies by Mindlin plate theory are consistent with that of from finite element analyses, but there are great deviations from the calculated resonant frequencies by thin plate theory, and that, the deviations become greater with increase of thickness of plates. With increase of the thickness of the plate, the errors of the calculated fundamental resonant frequency between by thin plate theory and by using finite element method increase, especially, the errors at the higher order resonant frequencies increase rapidly.

It still can be seen from the Table 1 that the maximal error of the fundamental resonant frequency is 44%, the maximal errors of the second and the third resonant frequency, respectively, are 109%, 173% by comparison of the calculated by thin plate theory and by using finite element method. However, comparing of the calculated by the Mindlin plate theory and by using finite element method, the maximal error of the fundamental resonant frequency

Table II. The calculated nodal circles of each vibrational mode.

| h | n | Frequencies (kHz) | | | Nodal circles | | | | | | | | |
|---|---|---|---|---|---|---|---|---|---|---|---|---|---|
| | | $f_M$ | $f_K$ | $f_A$ | $R_M$ | | | $R_K$ | | | $R_A$ | | |
| | 1 | 25.41 | 28.88 | 25.64 | 16.8 | | | 17.0 | | | 16.8 | | |
| 8 | 2 | 82.23 | 123.79 | 85.38 | 9.9 | 21.1 | | 9.8 | 21.0 | | 10.0 | 20.9 | |
| | 3 | 144.24 | 282.74 | 154.15 | 6.4 | 15.1 | 22.6 | 6.4 | 14.8 | 22.3 | 6.4 | 15.2 | 22.4 |
| | 1 | 30.06 | 36.10 | 30.33 | 16.9 | | | 17.0 | | | 16.7 | | |
| 10 | 2 | 90.46 | 154.74 | 93.64 | 10.0 | 21.1 | | 9.8 | 21.0 | | 10.2 | 20.9 | |
| | 3 | 150.59 | 353.43 | 158.80 | 6.6 | 15.1 | 23.6 | 6.4 | 14.8 | 22.3 | 6.3 | 15.8 | 22.9 |
| | 1 | 34.01 | 43.31 | 34.35 | 16.8 | | | 17.0 | | | 16.6 | | |
| 11 | 2 | 95.54 | 185.68 | 99.08 | 9.8 | 21.9 | | 9.8 | 21.0 | | 10.4 | 21.0 | |
| | 3 | 149.40 | 424.11 | 155.71 | 7.2 | 15.1 | 24.9 | 6.4 | 14.8 | 22.3 | 6.1 | 16.7 | 24.2 |

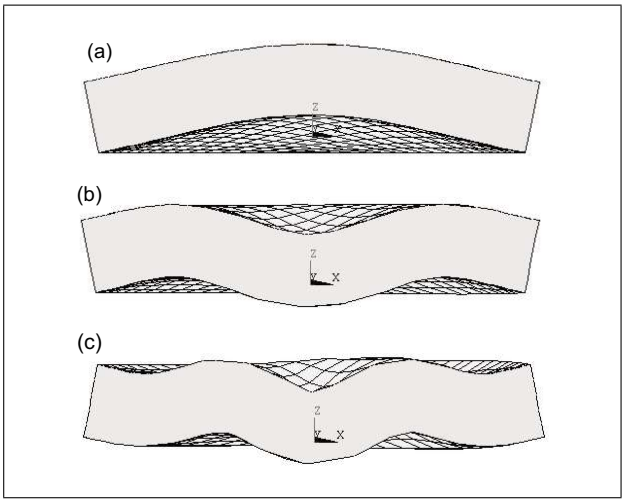


Figure 1. Modal patterns of the thick plate (the first three modes). (a) $n = 1$, (b) $n = 2$, (c) $n = 3$.

is only 3%, and the maximal errors of the second and the third resonant frequency, respectively, are 5%, 9%.

Table II shows the nodal circulars $R_A$, $R_M$ and $R_K$ calculated by using finite element method, by equation (12) and by thin plate theory, respectively, for three different thickness (8 mm, 10 mm, 12 mm) with the same radius ($a = 25$ mm) of plates at the free edge. Taking the 8mm thickness plate as an example, the first, second, and third order vibrational modes, respectively, are shown in Figures 1a to 1c. Figures 2a to 2c, Figures 3a to 3c and Figures 4a to 4c, respectively, are its relative displacement distributions versus diameter calculated by using finite element method, by equation (12) and by thin plate theory. It can be seen from the above Table II and the Figures that the nodal circulars calculated by equation (12) and by using finite element method are quite close, and the contours of relative displacement distributions corresponding to each calculation method are all similar. However, for the plates with different thickness but with the same radius, the nodal circulars calculated by thin plate theory are in the same position although their resonant frequencies are different. This is due to that thin plate theory neglects shear deformation and reduces a three-dimensional problem to a two-dimensional one.

Table III. The measured resonant frequencies of the two thick plates $h$ (mm).

| h | n | $f$ | $f_M$ | $f_K$ | $f_A$ |
|---|---|---|---|---|---|
| | 1 | 27.77 | 25.41 | 28.88 | 25.64 |
| 8 | 2 | 82.62 | 82.23 | 123.79 | 85.38 |
| | 3 | 150.82 | 144.24 | 282.74 | 154.15 |
| | 1 | 30.08 | 32.10 | 39.71 | 32.41 |
| 11 | 2 | 94.54 | 97.27 | 170.21 | 96.56 |
| | 3 | 155.46 | 150.55 | 388.77 | 157.80 |

## 4. Experimental configuration

In order to validate, two steel thick plates are fabricated, both of the radius of the plates are $a = 25$ mm, and their thicknesses are 8 mm and 11 mm, respectively, as shown in Figures 5a and 5b. The first three resonant frequencies of the two plates are tested.

The Experimental setup for frequency measurement is shown in Figure 6. T1 and T2 are piezoelectric ceramics transmitter and receiver. The diameters and the thickness of T1 and T2, respectively, are 10 mm, 2 mm and 5 mm, 1 mm. The resonant frequencies of T1 and T2 should be far away from those of the thick plates to be measured. From the given geometrical dimensions, it is obvious that the fundamental resonant frequencies of the transmitter and receiver are far higher than that of the thick plates to be measured. Therefore, the transmitter and receiver have little effect on the performances of the plates. T1 and T2 are attached to the opposite sides at the two edges of the plate, as shown Figure 6. The edge of the tested plate is free. Keep the magnitude of the excitation signal constant and continuously change the values of frequency from the generator in the process of the experiment, the corresponding frequency to the received greatest amplitude signal by the receiver just are the resonant one of the plate. The tested results are shown in Table III, where $n$ denotes the modal order number of the plate, $f$, $f_M$, $f_K$ and $f_A$ are the measured resonant frequencies, the calculated frequencies by

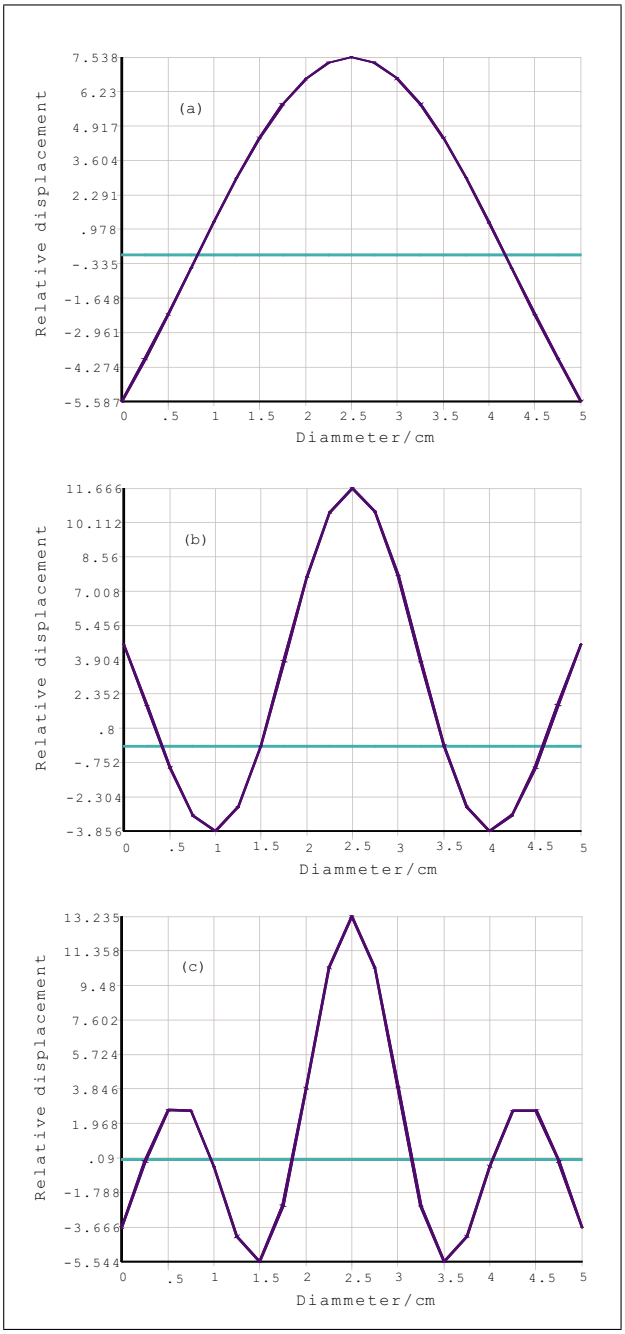


Figure 2. The calculated relative displacement distributions versus diameter by ANSYS with the 8 mm thickness plate (a) $n = 1$, (b) $n = 2$, (c) $n = 3$.

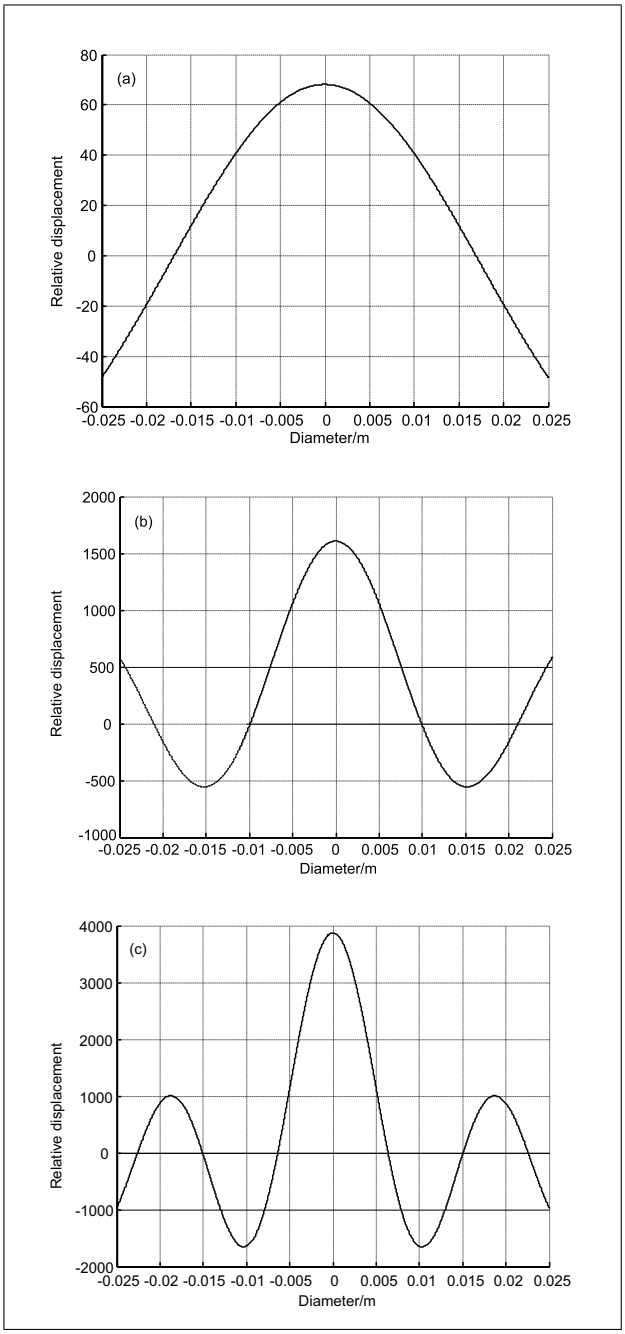


Figure 3. The calculated relative displacement distributions versus diameter by equation (12) with the 8 mm thickness plate (a) $n = 1$, (b) $n = 2$, (c) $n = 3$.

the presented analytical method, by thin plate theory and by using finite element method, respectively (as shown in Table I). It can be seen that the tested frequencies $f$ of the plates are in good agreement with those of the calculated ones $f_M$ and $f_A$. The reason why frequencies $f_K$ are higher than the tested frequencies $f$ is that thin plate theory neglects shear deformation and enlarges rigidity of the plates. The errors between the measured frequencies and the calculated ones by thin plate theory for the thickness of 11 mm plate are greater than those of the thickness of 8 mm plate. The errors of the measured frequencies may be from the standard values of the plate material parameters, which are different from those of the practical values of the material.

## 5. Conclusions

The purpose of this paper is to design a thick plate in flexural vibration at certain operating frequency with its boundary conditions being free, simply supported and clamped. To sum up the above analyses, the following conclusions can be drawn.

1. Thin plate theory, that is the hypothesis of Kirchhoff's, neglects shear deformation and enlarges rigidity of the

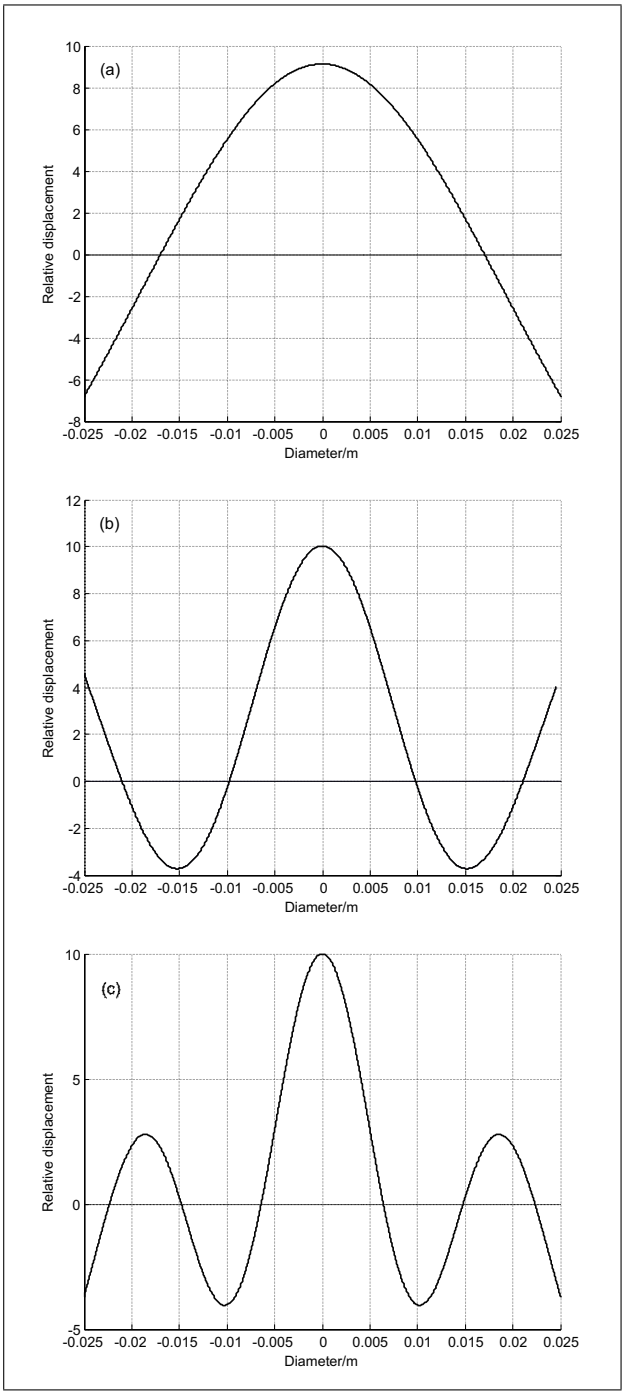


Figure 4. The calculated relative displacement distributions versus diameter by thin plate theory with the 8mm thickness plate (a) $n = 1$, (b) $n = 2$, (c) $n = 3$.

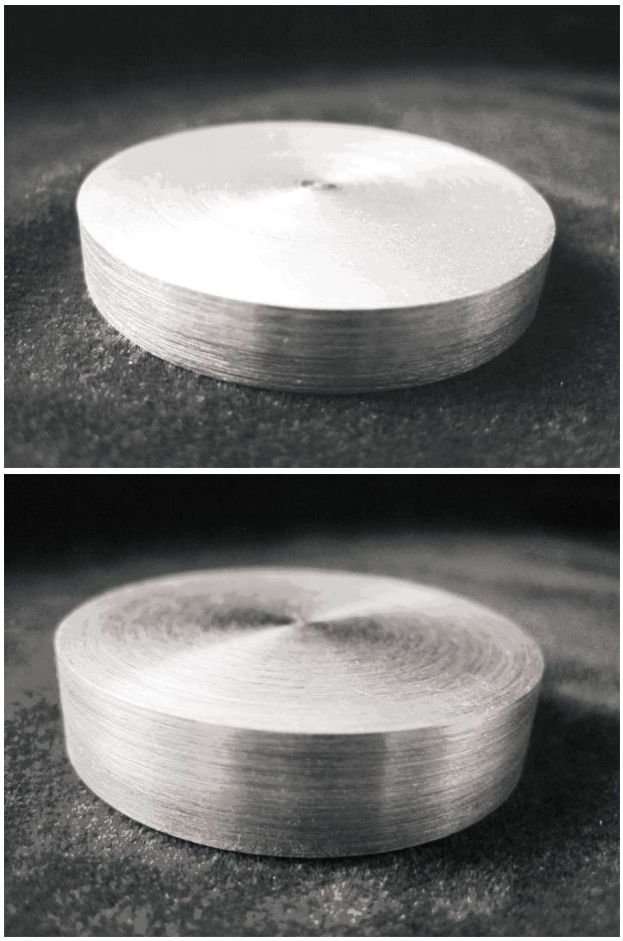

Figure 5. Two different thickness of the thick plates.

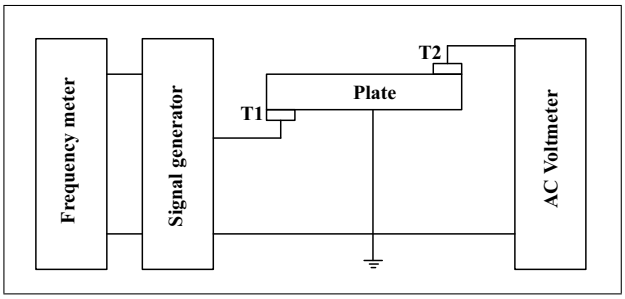


Figure 6. Setup for frequency measurement.

plates, and is mainly applicable for design of thin plates with small ratio of thickness to length. For a thick plate, the greater its ratio of thickness to length, the greater the error of frequency between the calculated by thin plate theory and the tested will be.

2. Thin plate theory reduces the three-dimensional problem to a two-dimensional one, therefore, for different thickness with the same radius of the plates, the nodal circulars calculated by thin plate theory are in the same position although their resonant frequencies are different.
3. The expressions of the transverse and the radial displacements, and the frequency equations based on Mindlin plate theory with three boundary conditions (free, simply supported, and clamped) of a thick plate in flexural vibration are derived.
4. The calculated resonant frequencies by the presented frequency equations and by using finite element method are consistent with those of the tests. The presented analytical method can be used for design of thick plates in flexural vibration which can withstand higher mechanical strength and obtain very large mechanical displacement amplitudes.

**Acknowledgement**

This work is supported by the National Natural Science Foundation of P. R. China (Grant No. 11374201).

**References**

[1] I. González, J. Rodríguez, I. Garmendia, J. A. Gallego: Application of high intensity air-borne ultrasound for debubbling liquid coating layers. Ultrason. **44** (2006) 529–532.

[2] G. Rodríguez, E. Riera, J. A. Gallego, V. M. Acosta, A. Pinto, I. Martínez, A. Blanco: Experimental study of defoaming by air-borne power ultrasonic technology. Phys. Proc. **3** (2009) 135–139.

[3] J. A. Gallego, G. Rodríguez-Corral, L. Gaete-Garreton: An ultrasonic transducer for high power applications in gases. Ultrason. **16** (1978) 267–271.

[4] E. Riera, J. A. Gallego, T. J. Mason: Airborne ultrasound for the precipitation of smokes and powders and the destruction of foams. Ultrason. Sonochem. **13** (2006) 107–116.

[5] A. Barone, J. A. Gallego: Flexural vibrating free-edge plates with stepped thickness for generating high directional ultrasonic radiation. J. Acoust. Soc. Am. **51** (1972) 953–959.

[6] J. A. Gallego: Axisymmtric vibrations of circular plates with stepped thickness. J. Sound Vib. **26** (1973) 411–416.

[7] E. Ventsel, K. Theodor: Thin plates and shells: theory, analysis, and applications. Marcel Dekker, New York, 2001.

[8] J. A. Gallego, G. Rodriguez, S. E. Riera, F. V. Martinez et al.: A macrosonic system for industrial processing. Ultrason. **38** (2000) 331–336.

[9] J. A. Gallego, G. Rodríguez, V. Acosta, E. Riera: Power ultrasonic transducers with extensive radiators for industrial processing. Ultrason. Sonochem. **17** (2010) 953–964.

[10] J. A. Gallego, G. Rodríguez, J. C. Gálvez, T. S. Yang: A new high-intensity ultrasonic technology for food dehydration. Drying Tech. **17** (1999) 597–608.

[11] J. A. Gallego, L. Elvira, G. Rodríguez: A power ultrasonic technology for deliquoring. Ultrason. **41** (2003) 255–259.

[12] E. Riera, J. A. Gallego, G. Rodríguez, L. Elvira, I. González: Application of high-power ultrasound to enhance fluid/solid particle separation processes. Ultrason. **38** (2000) 642–646.

[13] R. D. Mindlin: Influence of rotary inertia and shear on flexural motions of isotropic, elastic plates. Trans. ASME, J. Appl. Mech. **18** (1951) 31–38.